JOURNAL OF VIROLOGY, June 1996, p. 3636–3644 Vol. 70, No. 6
0022-538X/96/$04.00+0

Selection and Characterization of Replication-Competent Revertants of a Rous Sarcoma Virus *src* Gene Oversplicing Mutant

LEI ZHANG, SAMANTHA B. SIMPSON, AND C. MARTIN STOLTZFUS*

Department of Microbiology, University of Iowa, Iowa City, Iowa 52242

Received 29 June 1995/Accepted 12 March 1996

All retroviruses require both unspliced and spliced RNA for a productive infection. One mechanism by which Rous sarcoma virus achieves incomplete splicing involves suboptimal *env* and *src* 3′ splice sites. We have previously shown that mutagenesis of the nonconsensus *src* polypyrimidine tract to a 14-nucleotide uninterrupted polypyrimidine tract results in an oversplicing phenotype and a concomitant defective replication in permissive chicken embryo fibroblasts. In this report, we show that splicing at the *src* 3′ splice site (3′ss) is further negatively regulated by the suppressor of *src* splicing *cis* element which is located approximately 100 nucleotides upstream of the *src* 3′ss. The increase in splicing at the *src* 3′ss results in a corresponding increase in splicing at a cryptic 5′ss within the *env* gene. Two classes of replication-competent revertants of the *src* oversplicing mutant (pSAP1) were produced after infection, and these mutants were characterized by molecular cloning and sequence analysis. Class I revertants are transformation-defective revertants in which the *src* 3′ss and the *src* gene are deleted by homologous recombination at several different sites within the imperfect direct repeat sequences that flank the *src* gene. Cells infected with these transformation-defective revertants produce lower levels of virus particles than cells infected with the wild-type virus. Class II revertants bear small deletions in the region containing the branchpoint sequence or polypyrimidine tract of the *src* 3′ss. Insertion of these mutated sequences into pSAP1 restored inefficient splicing at the *src* 3′ss and efficient replication in chicken embryo fibroblasts. All of these mutations caused reduced splicing at the *src* 3′ss when they were tested in an in vitro splicing system. These results indicate that maintenance of a weak *src* 3′ss is necessary for efficient Rous sarcoma virus replication.

Most eukaryotic mRNAs are synthesized as precursors which undergo a splicing process. A conserved 5′ splice site (5′ss) and a 3′ splice site (3′ss), which includes the branchpoint sequence (BPS), the polypyrimidine tract (PPT), and the 3′ cleavage site, are necessary but not sufficient for accurate and efficient splicing. Many cellular factors and *cis*-acting elements have been found to play roles in the regulation of splice site strength and in selection of alternative splice sites. Regulated and alternative splicing may increase the coding capacity of a gene and allow gene expression in a tissue-specific or development-specific manner (for reviews, see references 12, 16, 17, and 28).

Retroviruses have evolved incomplete splicing to preserve a pool of unspliced RNA, which is required to serve three essential functions: (i) progeny virus particle packaging, requiring genomic RNA; (ii) expression of *gag* and *pol* genes, requiring mRNA; and (iii) splicing of *env* subgenomic mRNA and auxiliary subgenomic mRNAs, requiring pre-mRNA (7). Several mechanisms are employed by retroviruses to achieve incomplete splicing. First, retroviruses maintain weak splice sites to avoid efficient splicing (10, 14, 30, 44). Second, *cis* elements other than those at splice sites themselves are used to regulate the efficiency of splicing at particular splice sites (1, 4, 18, 19, 32). Third, complex retroviruses encode regulatory proteins, such as the human immunodeficiency virus type 1 Rev protein, to facilitate transport of unspliced and singly spliced viral mRNAs from the nucleus to the cytoplasm. Simple retroviruses, such as avian and murine leukemia viruses, do not encode such a transport protein and depend solely on host factors interacting with the viral *cis* elements to control the levels of unspliced and spliced RNA (for reviews, see references 8 and 31).

Rous sarcoma virus (RSV), a replication-competent oncogenic avian retrovirus which expresses the oncogene *src*, is an excellent system for studying RNA splicing by simple retroviruses. About 30% of the RSV RNA is spliced from a single 5′ss at nucleotide (nt) 398 to either a 3′ss at nt 5078 or a 3′ss at nt 7054 to form approximately equimolar amounts of *env* and *src* mRNA, respectively (see Fig. 1). The RSV *env* 3′ss has a consensus PPT with 10 consecutive pyrimidines; however, its BPS has been shown to be weak. A mutation which activated a more efficient alternative branchpoint resulted in overproduction of spliced *env* mRNA. Upon passage of this replication-defective mutant, replication-competent revertants with suppressor mutations either within the BPS or in the positive exon element downstream of the *env* 3′ss were selected (10, 13, 14). Such purine-rich exon splicing enhancer elements have been found in a number of genes, including the 3′-terminal *tat*/*rev* exon of human immunodeficiency virus type 1 RNA (2, 9, 34, 40, 42). In addition to the weak *env* 3′ss, two *cis*-acting elements that negatively regulate RSV splicing in chicken embryo fibroblasts (CEF) have been found. First, a negative regulator of splicing element located in the *gag* gene acts to inhibit production of both *env* and *src* mRNAs (4, 32). In HeLa cell nuclear extracts, the pre-mRNA containing the negative regulator of splicing element has been shown to form abnormally large, nonproductive ribonucleoprotein complexes containing U1, U2, U11, and U12 (11). Second, the *src* suppressor of splicing (SSS), located upstream of the *src* 3′ss, specifically inhibits *src* splicing (5, 18). The SSS element appears to interact with a cellular factor or factors which are present in per-

* Corresponding author. Phone: (319) 335-7793. Fax: (319) 335-9006. Electronic mail address: cmstoltz@vaxa.weeg.uiowa.edu.

missive chicken cells but not in nonpermissive mammalian cells (3).

In contrast to the *env* 3′ss, the putative *src* BPS, which is located 18 nt upstream of the *src* 3′ cleavage site, matches six of the seven bases of the consensus sequence (YNYURAC; branchpoint underlined) (45); the *src* PPT, however, is interrupted by four to five purines. We have previously reported that mutagenesis of the nonconsensus PPT to an uninterrupted 14-nt PPT (see Fig. 2C) resulted in oversplicing at the *src* 3′ss. Concomitantly, a cryptic 5′ss at nt 5237 was activated. This interference with balanced splicing causes a defect in virus replication in permissive CEF (44). In this study we have characterized two classes of replication-competent revertants of the *src* gene oversplicing mutant and show that the presence of an inefficient *src* 3′ss is necessary for efficient RSV replication.

MATERIALS AND METHODS

Plasmid constructs. The nonpermuted RSV (Prague A strain) DNA clone pJD100 contains an infectious and transformation-competent DNA provirus (a gift from J. T. Parsons, Department of Microbiology, University of Virginia, Charlottesville). pSAP1, which contains mutations within the *src* PPT, was constructed as described previously (44). Construction of the SSS mutant pPM87G was described elsewhere (3) (see Fig. 1A). pSAP2 was constructed by replacing the *Sac*I-*Xho*I fragment (nt 6865 to 6983) in pSAP1 with the corresponding fragment isolated from pPM87G, which contains a C-to-G mutation at nt 6887 within the SSS region.

Construction of riboprobe templates p5′XH1, pRES1, and pRES2 has been described previously (32, 44). Riboprobe template pRES4 was constructed by replacing the wild-type *Xho*I-*Nco*I fragment (nt 6983 to 7127) in the pRES1 clone with the corresponding fragment isolated from the suppressor mutant pSPR1 (see below). Riboprobe template pSRCBX was cloned by insertion of a *Xba*I-*Bgl*II fragment (nt 6861 to 7736) from pJD100 into pSPT19 which had been digested with *Xba*I and *Bam*HI.

Cloning and sequence analysis of pSAP1 revertants. (i) Class I revertants. To clone the revertant viral DNA, reverse transcription PCR was carried out as described previously (44). cDNA was synthesized by using Moloney murine leukemia virus reverse transcriptase (Bethesda Research Laboratories, Inc., Gaithersburg, Md.) in the presence of random hexamers (Pharmacia Biotech Inc., Piscataway, N.J.). The sense primer S36 (5′-GCAGTCTAGAGCTCAGT TATAATAATCC-3′; nt 6857 to 6884) and the antisense primer A41 (5′-GC GATGCGGAATTCAGTG-3′; nt 9251 to 9234) were used to synthesize the DNA fragments containing the deletion junction sites within the genomes of the transformation-defective (*td*) revertants (see Fig. 2A). The PCR products were digested with *Sac*I (nt 6865) and *Eco*RI (nt 9238) and ligated into pBluescript II KS (Stratagene, La Jolla, Calif.) which had been digested with *Sac*I and *Eco*RI. These clones were then sequenced by using the M13 primer (27). The clones containing sequences different from those of the original mutant pSAP1 (see above) were selected and given the designations pBSETD1, pBSETD2, and pBSETD3 (see Fig. 2B). The *Sac*I-*Eco*RI fragments (nt 6865 to 9238) in pBSETD1 and pBSETD2 were isolated and substituted into pSAP1 to generate pSTD1 and pSTD2.

(ii) Class II revertants. The cloning strategy is similar to that for class I revertants except that sense primer S36 and antisense primer A1 (5′-TCTTGCT GCTCCCCATGGTGGT-3′; nt 7144 to 7123) were used to synthesize the DNA fragments containing the *src* 3′ss and its flanking sequences (see Fig. 2A). The PCR products were digested with *Sac*I (nt 6865) and *Nco*I (nt 7127) and ligated into the corresponding region of pBSE, which was constructed by ligating the *Sac*I-*Eco*RI fragment (nt 6865 to 9238) from pJD100 into the *Sac*I and *Eco*RI sites of pBluescript II KS. The clones containing sequences different from those of pSAP1 were selected and given the designations pBSEPR1, pBSEPR2, pBSEPR3, and pBSEPR4 (see Fig. 2C). The *Sac*I-*Eco*RI fragments (nt 6865 to 9238) in pBSEPR1, pBSEPR2, and pBSEPR4 were isolated and substituted into pSAP1 to generate pSPR1, pSPR2, and pSPR4, respectively.

(iii) In vitro splicing minigene constructs. The in vitro splicing minigene construct pRSVWT, which was previously called pRSV1176 (1), contains the wild-type RSV 5′ss and *src* 3′ss. pRSAP1 was constructed by replacement of the *Xho*I-*Nco*I fragment (nt 6983 to 7127) in pRSVWT with the corresponding fragment isolated from pSAP1. The same region in pRSVWT was also replaced by the corresponding fragments isolated from pBSEPR1, pBSEPR2, pBSEPR3, and pBSEPR4 to generate pRSPR1, pRSPR2, pRSPR3, and pRSPR4, respectively.

Cell culture, RSV infection, and transfection assays. Secondary CEF isolated from embryonated eggs that were negative for both group-specific antigen and chicken helper factor (SPAFAS, Inc., Norwich, Conn.) were cultured in Medium 199 (Bethesda Research Laboratories, Inc., Gaithersburg, Md.) supplemented with 10% (vol/vol) tryptose phosphate broth and 5% (vol/vol) calf serum. DNA transfections were performed by the calcium phosphate coprecipitation procedure essentially as previously described (38). The DNA precipitates were added to culture medium lacking tryptose phosphate broth. Two hours later, the cells were shocked with 30% dimethyl sulfoxide for 2 min. RSV infection was carried out by passage of the transfected cells every 3 to 4 days. After two passages, the cells were further passaged by dilution with three parts of nontransfected CEF.

RNA isolation, RNase protection assays, and Northern (RNA) blot analyses. Total cellular RNA was harvested by the guanidine hydrochloride method (33). RNase protection assays were carried out as described previously (5) except that the RNase digestions were performed for 30 min at room temperature with 500 U of RNase T_1 (Boehringer-Mannheim Biochemicals, Indianapolis, Ind.) per ml and 3 μg of RNase A (Sigma Chemical Co., St. Louis, Mo.) per ml. Quantification of radioactive bands on the gels was conducted with the AMBIS image analysis system (AMBIS, Inc., San Diego, Calif.). Northern blot analysis was performed essentially as described by Sambrook et al. (26). Total RNA (5 μg) was denatured, separated on a 1.2% formaldehyde–agarose gel, and transferred to GeneScreenPlus membranes (DuPont, Wilmington, Del.). The membrane-bound RNA was hybridized to 2×10^6 cpm of ^{32}P-labeled riboprobes (see Fig. 4) in hybridization buffer (50% formamide, 10% dextran sulfate, 1% sodium dodecyl sulfate [SDS], 1 M NaCl, and 100 μg of denatured sheared salmon sperm DNA per ml) at 65°C. The membranes were then washed twice with 2× SSC (1× SSC is 0.15 M NaCl plus 0.015 M Na citrate) (pH 7) for 5 min at room temperature, twice with 2× SSC–1% SDS for 30 min at 75°C, and twice with 0.1× SSC for 5 min at room temperature.

Reverse transcriptase assays. The reverse transcriptase (RTase) assays were carried out as described previously (44).

In vitro splicing. ^{32}P-labeled splicing substrates were synthesized in vitro from *Nae*I-linearized plasmids. Preparation of HeLa cell nuclear extracts and the in vitro splicing reaction were conducted essentially as described previously (1).

RESULTS

Suboptimal *src* 3′ss and the SSS element act together to limit *src* splicing efficiency. We have previously reported that optimizing the PPT of the *src* 3′ss results in a dramatic increase in *src* splicing and a significant delay in virus production in permissive chicken cells (44). Besides the suboptimal *src* 3′ss, another element, the SSS, is located approximately 100 nt upstream of the RSV *src* 3′ss (5, 18). We have proposed that the SSS element and the suboptimal *src* 3′ss act together to limit splicing efficiency at the *src* 3′ss. To test whether the SSS element inhibits splicing at the improved *src* 3′ss, we constructed a double mutant (pSAP2) with both a C-to-G mutation at nt 6887 within the SSS element and the improved *src* PPT mutations (Fig. 1A). It has been found that this single point mutation in RSV is sufficient to cause an approximately twofold increase in *src* splicing (3, 5). To test the effect of the SSS element in the context of the improved *src* PPT, the improved PPT mutant (pSAP1), the single SSS mutant (pPM87G), and the double mutant (pSAP2) were transfected into CEF and RNase protection assays were performed (Fig. 1B). The quantitative data obtained from multiple RNase protection assays demonstrate increases in splicing of approximately two- and fourfold at the *src* 3′ss with the single SSS mutant (pPM87G) and the improved PPT mutant (pSAP1), respectively (Table 1). The combination of the two mutations (pSAP2) resulted in an approximately fivefold increase in splicing at the *src* 3′ss, suggesting that the SSS element still functions to inhibit splicing even in the presence of an optimized *src* 3′ss. Thus, the suboptimal *src* PPT and the SSS element appear to act together to limit splicing at the *src* 3′ss. Furthermore, the increase of splicing at the *src* 3′ss in pSAP2 was concomitant with an increase of splicing at the cryptic 5′ss (Table 1). This result reinforced our previous conclusion that activation of the cryptic 5′ss is correlated with the strength of the *src* 3′ss (44).

Molecular cloning and sequence analysis of the class I and class II revertants. Our previous results suggested that two classes of replication-competent revertants arose after passage of the cells transfected with the *src* PPT mutant pSAP1. Class I revertants are *td* deleted viruses containing genomes of approximately 7.3 kb. Our previous data indicated that production of such revertants did not occur when cells transfected

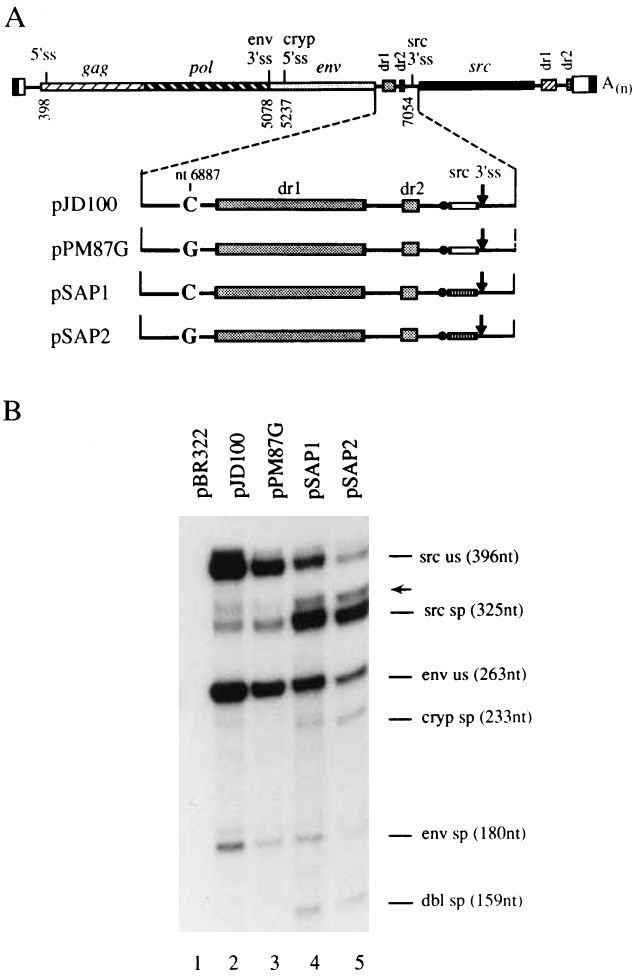

FIG. 1. The suboptimal *src* 3′ss and the upstream SSS element act together to limit *src* splicing. (A) Schematic representation of RSV genome and viral DNA constructs. The nucleotides are numbered according to the RSV Prague C sequence. cryp, cryptic splice site. The closed circle indicates the BPS of the *src* 3′ss. The open box and the hatched box indicate the wild-type and optimized PPT sequences, respectively, which are shown in Fig. 2C. (B) Patterns of RNase protection assays which were performed as previously described (44). The pRES1 riboprobe was used to analyze RNA from mock (pBR322)-pJD100-, and pPM87G-transfected cells. The pRES2 riboprobe was used to analyze RNA from pSAP1- and pSAP2-transfected cells. The locations and the sizes of the resulting protected fragments are indicated on the right. The band marked with an arrow is an artifact resulting from incomplete RNase digestion. The relative amounts of viral RNA species are shown in Table 1. us, unspliced; sp, spliced; cryp, cryptic; dbl, double.

with the wild-type Prague A RSV clone (pJD100) were passaged in parallel (44). On the basis of previous reports, the deleted 2-kb region most likely is located between the direct repeat (dr) sequences flanking the *src* open reading frame (21, 37, 41). To confirm this and to characterize the precise site of the deletions, DNA fragments containing the presumptive deletion junction sites were cloned by using the S36 and A41 primer pair (Fig. 2A). The second class of revertants, class II revertants, contain genomes of 9.3 kb and may bear suppressor mutations that weaken the *src* 3′ss (44). To determine if this was the case, DNA fragments containing the *src* 3′ss and flanking sequences were cloned by using the S36 and A1 primer pair (Fig. 2A).

Total cellular RNA was isolated from chicken cells 12 days after transfection with the *src* PPT mutant pSAP1. cDNA was synthesized and PCR was performed with the two primer pairs (Fig. 2A) (see also Materials and Methods). The PCR products were analyzed by electrophoresis on 8% polyacrylamide gels. As expected, an approximately 500-bp fragment synthesized with the S36-A41 primer pair and an approximately 280-bp fragment synthesized with the S36-A1 primer pair were observed (data not shown). These fragments were isolated, digested with the appropriate restriction enzymes shown in Fig. 2A, and cloned into pBluescript II KS. Ten S36-A41-derived clones were sequenced (see Materials and Methods), and three different deletions, denoted TD1, TD2, and TD3, were found (Fig. 2B). These deletions were generated by homologous recombination at different sites within the upstream dr1 (5′dr1) and the downstream dr1 (3′dr1). A total of 14 S36-A1-derived clones were sequenced; 3 of them had original pSAP1 sequences, and 11 had the same 7-nt deletion in the *src* 3′ss (Fig. 2C). This small deletion, denoted PR1, results in a reduction in the length of the *src* PPT from 14 to 8 nt. To screen for revertants with suppressor mutations other than PR1, we sequenced clones derived from two other independent experiments in which CEF were transfected with pSAP1. As shown in Fig. 2C, three additional class II mutations, PR2, PR3, and PR4, were found. The PR2 and PR3 mutations contained small deletions of the PPT which reduced the length of the *src* PPT to 7 and 3 nt, respectively. In the PR4 mutation, the putative *src* BPS was completely deleted.

Revertants are replication competent in chicken cells. As demonstrated above, the two classes of revertants either completely lack the *src* 3′ss (class I) or are mutated in the PPT or BPS of the *src* 3′ss (class II). We reasoned that these mutations may compensate for the oversplicing phenotype caused by the improved *src* PPT mutations (pSAP1). To test the effects of these mutations on viral replication, we substituted the DNA fragments containing TD1, TD2, PR1, PR2, and PR4 muta-

TABLE 1. Relative amounts of viral RNA species in CEF transfected with RSV proviral DNA mutated within the SSS element and the *src* PPT[a]

Construct	% (±SD) of RNA molecules						
	Unspliced (genomic)	Single-spliced *env*	Single-spliced *src*	Cryptic single-spliced	Double-spliced	Total at cryptic 5′ss[b]	Total at *src* 3′ss[c]
pJD100	73.0 ± 3.9	12.5 ± 0.9	14.6 ± 3.4	ND	ND	ND	14.6 ± 3.4
pPM87G	62.9 ± 5.2	10.4 ± 0.5	24.6 ± 4.7	ND	2.1 ± 0.5	2.1 ± 0.5	26.8 ± 5.0
pSAP1	30.9 ± 0.3	7.1 ± 0.6	52.2 ± 2.3	3.4 ± 1.1	6.5 ± 0.8	9.8 ± 1.4	62.0 ± 0.9
pSAP2	20.7 ± 1.8	4.4 ± 0.7	57.5 ± 2.9	8.4 ± 0.8	8.8 ± 0.3	17.3 ± 0.9	74.8 ± 1.8
pSPR1	83.6 ± 2.1	10.0 ± 0.8	7.0 ± 2.1	ND	ND	ND	7.0 ± 2.1

[a] RNase protection assays and calculations were carried out as previously described (44). The values are based on averages of multiple determinations from at least two independent experiments. ND, not detected.
[b] Sum of relative amounts of cryptic single-spliced and double-spliced RNAs.
[c] Sum of relative amounts of single-spliced *src*, cryptic single-spliced, and double-spliced RNAs.

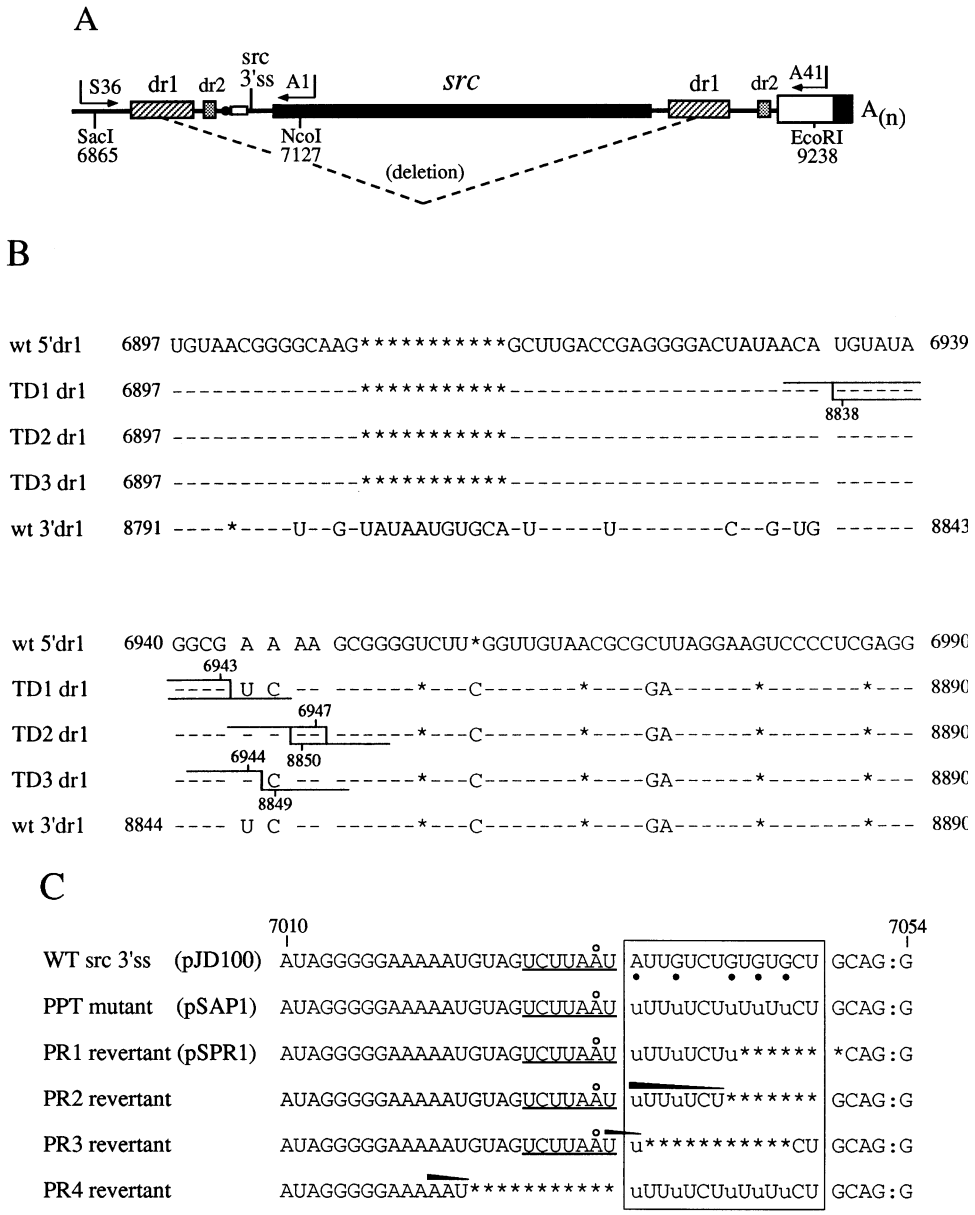

FIG. 2. Sequencing analysis of RSV revertants. (A) Schematic representation of the 3′ region of RSV genome and primers used for cloning revertant-derived viral DNA by reverse transcription PCR. Sense primer S36 and antisense primer A1 were used to synthesize DNA fragments containing the *src* 3′ss and its flanking sequences. The same sense primer (S36) and antisense primer A41 were used to synthesize DNA fragments containing the deletion junction sites within the *td* viral genomes. The PCR products were digested at the indicated restriction sites, and the resulting fragments were substituted for the corresponding sequences in pSAP1 (see Materials and Methods). (B) Alignment of the dr1 sequences and the crossover sites of the *td* revertants (class I). The bases in the boxes indicate overlapping regions present in the sequence of both endpoints. The missing bases are marked with asterisks. 5′dr1, upstream dr1; 3′dr1, downstream dr1; wt, wild type. (C) Nucleotide sequences of the class II revertants. The five purines, indicated by closed circles, within the boxed putative PPT in pJD100 (wild type [WT]) were replaced with uracils to generate the pSAP1 mutant (44). The open circles indicate the putative branchpoints. The nucleotides that agree with the consensus BPS are underlined. The deleted nucleotides in the revertants are marked with asterisks. The closed triangles indicate the short repeats which are found at the 3′ end of the deleted sequences. u, substituted uracil moiety.

tions for the homologous regions in pSAP1 to generate pSTD1, pSTD2, pSPR1, pSPR2, and pSPR4, respectively (see Materials and Methods). CEF were transfected with each of the clones, and the virion-associated RTase activities in the culture media were measured at various times posttransfection. The wild-type pJD100 clone and the *src* PPT mutant pSAP1 clone were included as controls in this assay. Since only a relatively small fraction of cells are transfected, the level of RTase activity primarily reflects virus production from cells in which virus has spread from the initially transfected cells.

Consistent with our previous observations (44), RTase activity in the culture medium of cells transfected with the wild-type pJD100 was detected beginning at 3 days after transfection whereas an approximately 2-day delay was observed before RTase was detected in the medium of the pSAP1-transfected cells (Fig. 3). As shown above by the sequence analysis of PCR products, a majority of the viral RNAs in the pSAP1-transfected cells contained either deletions (class I) or mutations in the region of the *src* 3′ss. Virus clones containing either the TD1 or TD2 mutations were replication competent;

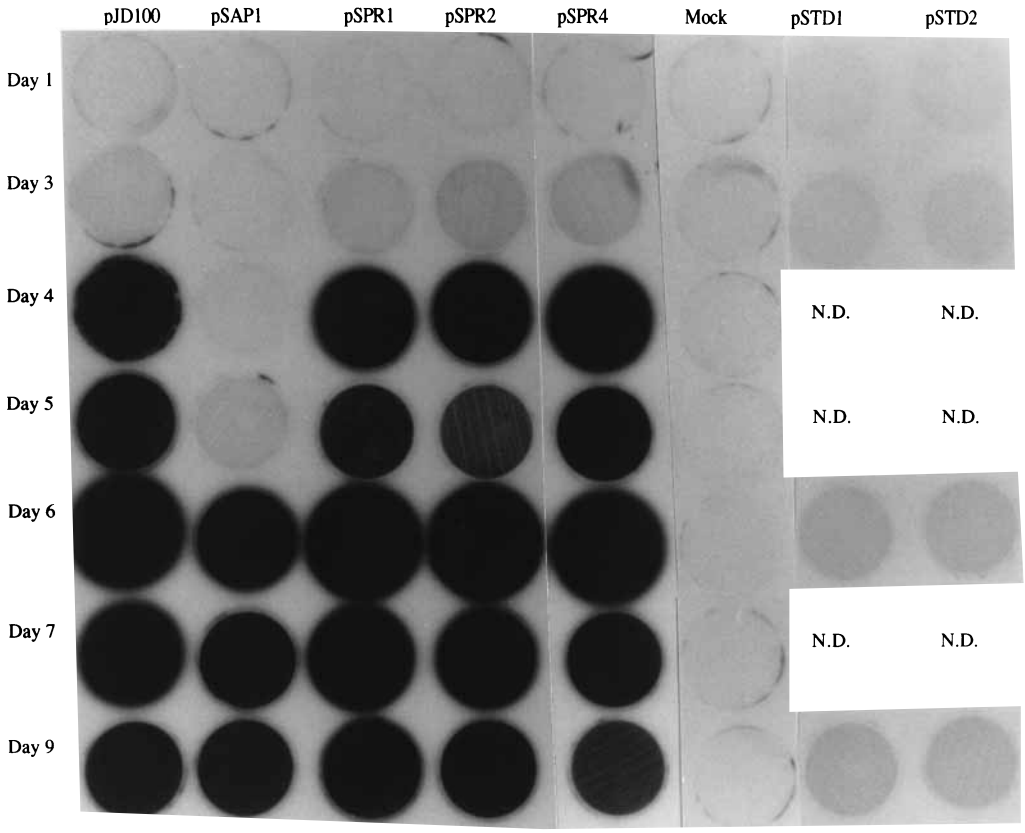

FIG. 3. The cloned revertants replicate with kinetics similar to that of the wild type. The mutations in pSAP1, pSPR1, pSPR2, pSPR4, pSTD1, and pSTD2 are shown in Fig. 2B and C. The construction of these clones is described in Materials and Methods. After CEF cells were transfected with viral DNA or with control DNA (mock), the culture medium was analyzed for RTase activity (44) at various times after transfection as shown in the figure. The incorporation of [α-^{32}P]TTP into trichloroacetic acid-precipitable material was detected by autoradiography. The cells were passaged on day 4 after the medium was harvested; this accounts for the lower RTase levels in the 5-day samples. Representative data are shown; this experiment was repeated three times with similar results. N.D., not determined.

their RTase activities in the culture medium, however, were 10- to 20-fold lower than that of the wild-type pJD100 (Fig. 3). As expected, cells were not transformed by these viruses (data not shown). In contrast, as shown in Fig. 3, virus clones containing the class II mutations (pSPR1, pSPR2, and pSPR4) replicated with kinetics similar to wild-type replication kinetics. Cells transfected with pSPR1 and pSPR2 were transformed at the same time and to approximately the same extent as cells transfected with the wild-type clone, whereas cells transfected with pSPR4 demonstrated much less transformation. These differences in transformation were correlated with the relative efficiencies of splicing at the *src* 3′ss (see next section).

To confirm that these viruses are indeed replication competent in CEF, we analyzed the viral RNA isolated from CEF 12 days posttransfection by Northern blot hybridization (Fig. 4). These RNAs were hybridized either with the p5′XH1 riboprobe, which hybridizes to the 5′ untranslated region in all RSV RNA species (lanes 1 to 6), or with the pSRCBX riboprobe, which hybridizes to the *Nco*I-to-*Bgl*II region (nt 7127 to 7736) within the *src* gene (lanes 7 to 12). In the wild-type pJD100-transfected cells, the 9.3-kb genomic RNA and the spliced *env* mRNA (4.7 kb) and *src* mRNA (2.7 kb) can be detected by using both probes (lanes 2 and 8). As observed previously (44), the RNA isolated from the pSAP1-transfected cells included a mixture of viral RNAs derived from at least two different viruses with different genome sizes (lane 3). The 9.3-kb RNA represents predominantly the genomic RNA of the class II revertants, while the 7.3-kb RNA represents the genomic RNA of the *td* revertants since the 7.3-kb RNA cannot be detected with the *src*-specific pSRCBX riboprobe (lane 9). As expected, the 9.3-kb genomic RNA in the pSPR1-transfected cells can be detected with both probes, and 7.3-kb RNA was not present (lanes 4 and 10). In the pSTD1- or pSTD2-transfected cells, the 7.3-kb genomic RNAs and the spliced *env* mRNAs (2.7 kb) were detected with the p5′XH1 riboprobe (lanes 5 and 6) but not with the pSRCBX riboprobe (lanes 11 and 12). This was expected since these RNAs lacked the *src* gene sequences. Surprisingly, in view of the relatively low levels of replication demonstrated by RTase assays (see Fig. 3), the viral RNA levels in the pSTD1- and pSTD2-transfected cells (lanes 5 and 6) were comparable to those of all other replicating viruses (lanes 2 to 4), indicating that, like the pSPR1 revertant, the *td* revertants are also replication competent and that by 12 days after transfection these viruses had spread throughout the culture. The RNAs tested in this experiment were isolated after serially diluted passage of the transfected cells, and therefore the viral RNA levels would be negligible if the viruses were replication defective. These results suggest the possibility that the replication defects of pSTD1 and pSTD2 may be posttranscriptional (see Discussion).

Class II mutations restore inefficient *src* splicing in vivo. We have shown that the pSPR1 and pSPR2 revertants contain shorter *src* PPTs and that these mutations restore efficient replication phenotypes in permissive CEF. We then tested

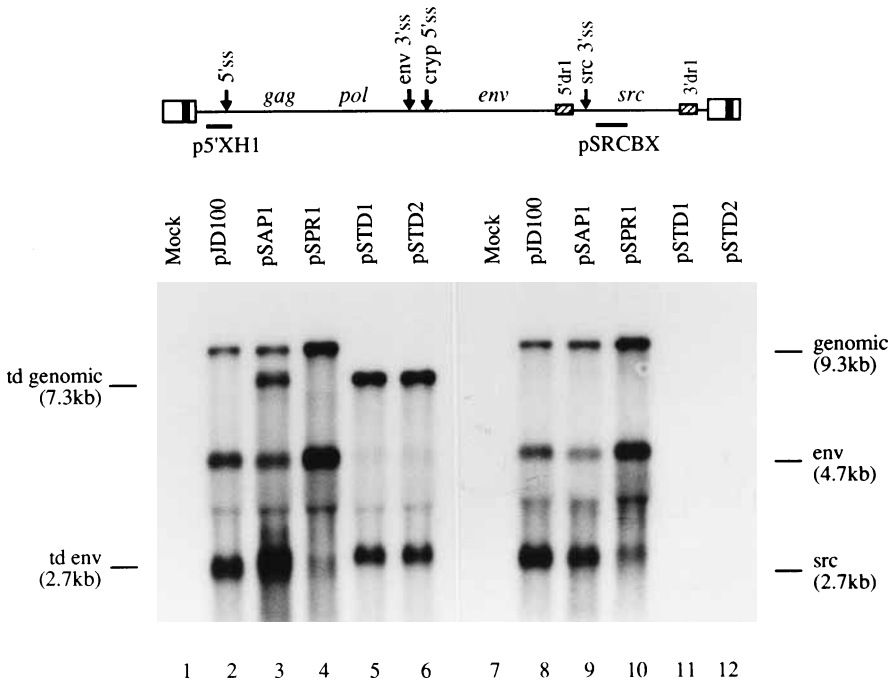

FIG. 4. Northern blot analysis of viral RNAs in wild-type-, *src* PPT mutant-, and recombinant revertant-infected cells. Total cellular RNAs were isolated 12 days posttransfection. Northern blot analysis was conducted as described in Materials and Methods. The membrane was hybridized with either the p5′XH1 riboprobe (lanes 1 to 6) or the pSRCBX riboprobe (lanes 7 to 12). The genomic (unspliced) and subgenomic (*env* and *src*) RNA species and their sizes are indicated. cryp, cryptic.

whether efficient virus replication correlates with inefficient viral RNA splicing. The Northern blot data shown in Fig. 4 suggested that inefficient splicing at the *src* 3′ss is restored in pSPR1 revertant-infected cells. Furthermore, no 7.3-kb RNA was detected in these cells, in contrast to the pSAP1-transfected cells (lane 3). Similar results were obtained for pSPR2 and pSPR4 revertant-infected cells (data not shown). To more accurately compare the efficiencies of *src* splicing, we used RNase protection analyses to compare the levels of viral RNA species in cells transiently transfected for 48 h with pJD100, pSAP1, or pSPR1 viral DNA (Fig. 5 and Table 1). As shown above, a significant increase in the level of spliced *src* mRNA, from 14.6% of the viral RNA in wild-type pJD100-transfected cells to 62.0% of the viral RNA in pSAP1-transfected cells, was observed (Fig. 5, lanes 3 and 4, and Table 1). Furthermore, as shown in Fig. 5 (lane 4), the strong *src* 3′ss in pSAP1 was associated with activation of a cryptic 5′ss at nt 5237 to produce cryptic single-spliced RNA and double-spliced RNA. The replication-competent pSPR1 revertant restored inefficient splicing at the *src* 3′ss (Fig. 5, lane 5). The *src* mRNA level was reduced from 52.2% in the pSAP1-transfected cells to only 7% in the pSPR1-transfected cells, and splicing at the cryptic 5′ss was no longer detectable (Table 1). We conclude, therefore, that inefficient splicing at the *src* 3′ss is restored in pSPR1-transfected cells.

Class II mutations are spliced inefficiently in vitro. To confirm that the changes in steady-state levels of *src* mRNA in infected cells were due to differences in splicing efficiency, we constructed the RSV splicing minigenes containing the *src* PPT mutation and the PR1 mutation. ^{32}P-labeled RNA substrates transcribed from the minigene templates were spliced in vitro for 2 h in HeLa cell nuclear extracts (see Materials and Methods) (Fig. 6A), and the reaction products were separated on a 7 M urea–4% polyacrylamide gel as shown in Fig. 6A. The amounts of radioactivity in the spliced-product bands were

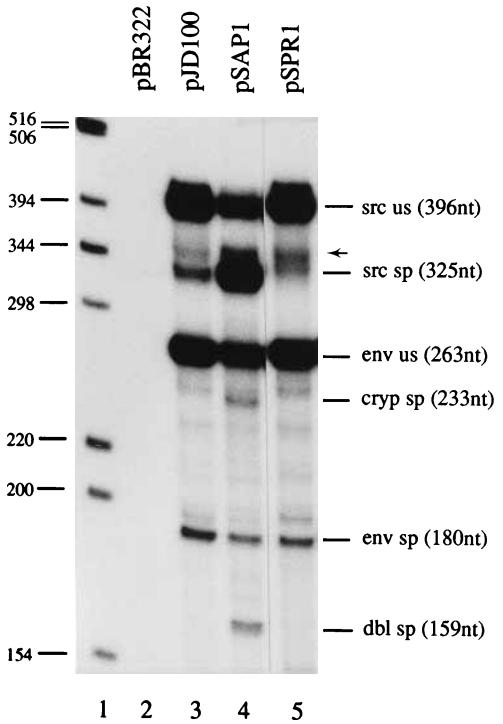

FIG. 5. The pseudorevertant restores inefficient splicing at the *src* 3′ss in CEF. Total cellular RNA (10 μg) isolated from transiently transfected CEF was analyzed by RNase protection assays as described in Materials and Methods. The pRES1 riboprobe was used to analyze RNA from the mock (pBR322)- and pJD100-transfected cells, and the compensatory pRES2 and pRES4 riboprobes were used to analyze RNA from pSAP1- and pSPR1-transfected cells, respectively. The locations and the sizes of the resulting protected fragments are indicated on the right. The band marked with an arrow is an artifact resulting from incomplete RNase digestion. Lane 1, 1-kb ladder marker. us, unspliced; sp, spliced; cryp, cryptic; dbl, double.

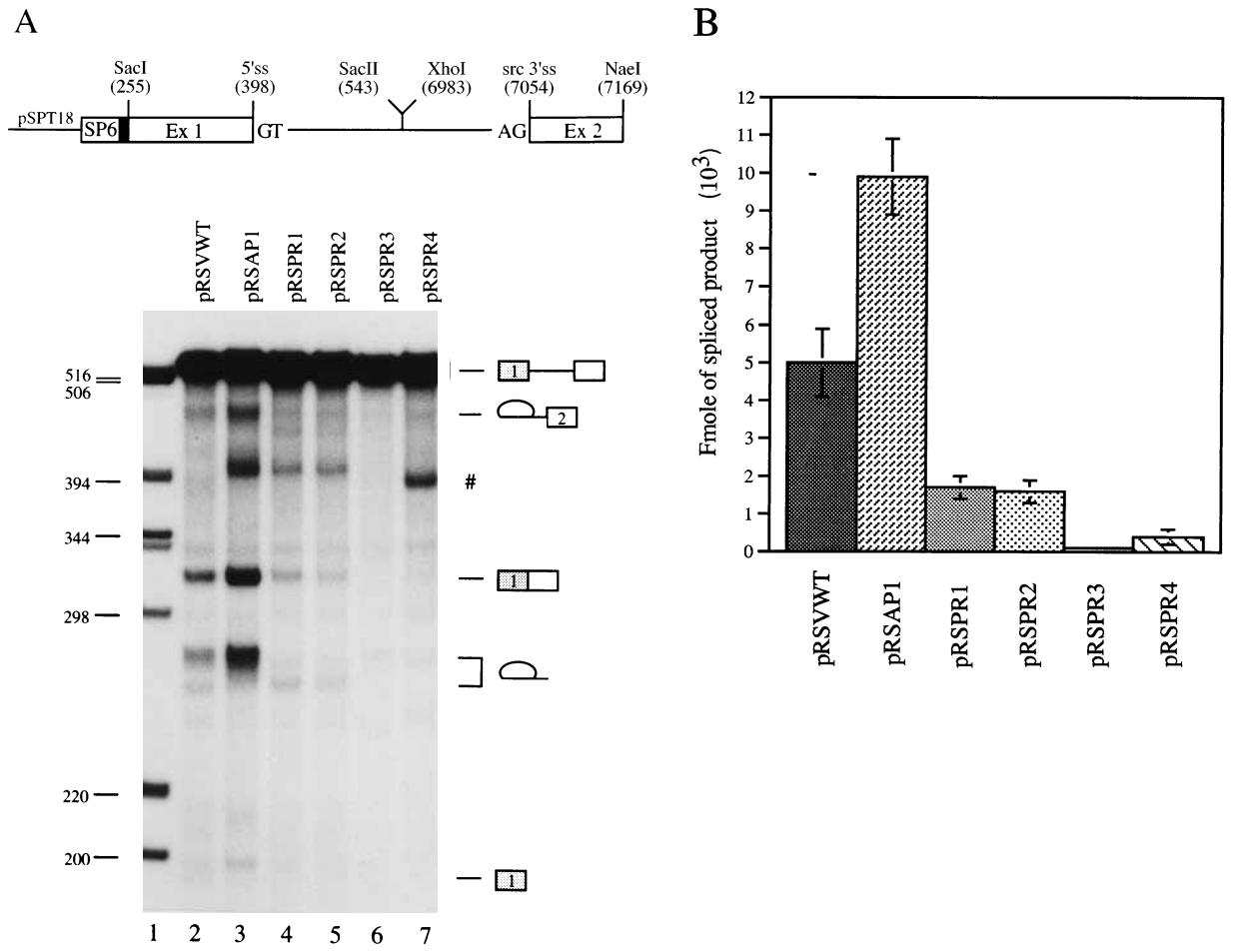

FIG. 6. Effects of the class II mutations on *src* splicing in a HeLa cell in vitro splicing system. (A) Patterns of in vitro splicing. The constructs for in vitro transcription and splicing are diagrammed at the top of the panel. These constructs were truncated at nt 7169, and the runoff transcripts driven by SP6 RNA polymerase were labeled with [^{32}P]UTP. Splicing reaction mixtures were incubated in HeLa cell nuclear extracts at 30°C for 2 h. RNAs were then purified, separated on a 4% polyacrylamide gel, and visualized by autoradiography. The structures of the RNAs are illustrated on the right. The bands marked with # are artifacts since they do not appear to represent any spliced products. They are not lariat intermediates since they do not undergo expected aberrant mobility shifts when electrophoresed on gels containing different percentages of polyacrylamide (data not shown). Lane 1, 1-kb ladder marker. Ex, exon. (B) Quantification of spliced products shown in panel A. The gels were scanned and quantitated with an AMBIS analysis system. The histograms indicate the levels of spliced products, which were calculated on the basis of the uridine content of each template. The error bars represent the standard deviations from four independent experiments.

quantitated with the AMBIS image analysis system and normalized to molar amounts of spliced product (Fig. 6B). At the 2-h point, the splicing efficiency of RNA containing the improved *src* PPT mutation (Fig. 6A, lane 3) was significantly higher than that of the wild-type RNA (lane 2), whereas RNA containing the PR1 suppressor mutation (lane 4) was spliced with an efficiency even lower than that of the wild-type RNA. Thus, both in vivo and in vitro splicing results indicate that the pSPR1 revertant contains an inefficient *src* 3′ss.

To determine the effects of other class II deletions on *src* splicing, we performed similar in vitro splicing assays in HeLa cell nuclear extracts. As expected, all of these mutations caused a significant reduction of splicing at the *src* 3′ss (Fig. 6). The splicing efficiency of RNA containing the PR2 mutation (Fig. 6A, lane 5) was comparable to that of RNA containing the PR1 mutation (lane 4). The splicing efficiency of RNA containing the PR3 mutation was extremely low (lane 6), reflecting the almost complete elimination of the PPT. Removal of the region containing the putative *src* BPS (PR4 mutation) caused a significant reduction in the splicing efficiency at the *src* 3′ss (lane 7), suggesting that this putative BPS is normally used in the RSV genome. The low level of spliced products detected may be generated by using an alternative nonconsensus BPS. The results indicate that the class II revertants achieve inefficient splicing by mutagenesis at the consensus *src* 3′ss present in the original PPT mutant to form a nonconsensus splice site.

DISCUSSION

Retroviruses are known to mutate at high rates, which allows them to adapt quickly to genetic and environmental changes (for reviews, see references 7 and 35). We have shown that when the *src* PPT is mutated to an uninterrupted 14-nt pyrimidine tract, this improved PPT causes an oversplicing phenotype and a defect in virus replication (44) (Fig. 3). Two classes of replication-competent revertants were rapidly selected after passage of the *src* PPT mutant. Among the four different class II mutations, the PR2, PR3, and PR4 mutations appear to arise by removal of nucleotides between short direct repeat sequences as shown in Fig. 2C; this type of deletion is common in retroviruses (22, 23). These deletions occur in regions (BPS and PPT) that are necessary for efficient splicing. RNA-RNA

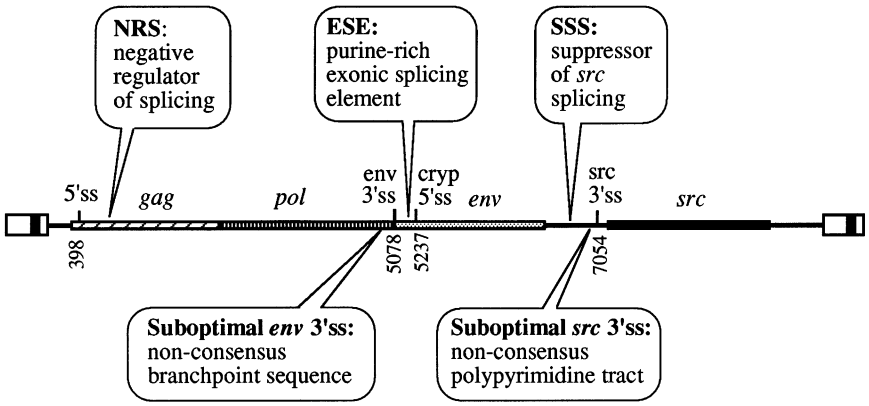

FIG. 7. Locations of known RSV splicing regulatory elements.

base pairing between the BPS and the U2 small nuclear ribonucleoprotein is important for subsequent splicing reactions (20, 39, 45). The functional strength of a PPT, which interacts with U2AF (43), has been shown to be correlated with its length and uridine content (24, 25). Thus, it appears that these class II mutations suppress the oversplicing phenotype in the pSAP1-transfected cells and restore efficient virus replication. Consistent with this interpretation, we showed that class II mutations restore inefficient splicing at the *src* 3′ss (Fig. 6) and that viruses affected by such mutations replicate more efficiently in chicken cells than does the pSAP-1 mutant (Fig. 3). We concluded from these results that the RSV *src* 3′ss, like the *env* 3′ss, is a weak splice site and that maintenance of this suboptimal splice site is necessary for efficient RSV replication. In addition, three other negative and positive *cis*-acting elements that regulate viral RNA splicing have previously been identified within the RSV genome. These are summarized in Fig. 7. We have shown in this study that splicing at the *src* 3′ss is inhibited by the SSS element in CEF even when the *src* 3′ss is optimized (Fig. 1). Thus, *cis*-acting elements at locations other than splice sites may also be required to further adjust the balance of splicing to the most favorable levels compatible with virus replication.

The class I *td* revertants arise by recombination at various positions within the dr sequences. RSV has two dr sequences flanking the *src* gene, and each copy consists of dr1 (approximately 100 nt) and dr2 (approximately 36 nt). The dr element has been shown to be necessary for virus replication (29). One copy of the dr element is sufficient for efficient virus replication, as demonstrated by many naturally occurring and recombinant avian retroviruses (6, 36). It was surprising that after placement of the single chimeric TD1 and TD2 dr elements into the viral genome, particle production was reduced to approximately 10% of that of the wild-type virus and the class II revertants (Fig. 3). It was also surprising that even though virus production was relatively low, the level of viral RNA in cells infected for 12 days with pSTD1 and pSTD2 was comparable to the wild-type virus level (Fig. 4). These results suggest that these clones may have a posttranscriptional replication defect. Included in these potential posttranscriptional functions is the reported role of the dr element as a *cis*-acting packaging signal (29). Since the homology of these dr sequences is only 80% and the resulting chimeric dr sequence is different from both of the wild-type dr sequences (Fig. 2B), it is possible that these differences in the dr sequence may significantly affect the function of the resulting chimeric dr element. It has been previously shown that even though RSV *td* mutants are the most commonly observed deletion mutants (15), the *td* mutants generated by homologous recombination between the *dr* sequences were not found as frequently as other *td* mutants when Prague B RSV was subjected to long-term high-multiplicity passage (37). Of the *td* mutants derived from Prague RSV strain (21, 37) whose sequences have been determined, only pATV9 was found to be generated by homologous recombination within the shorter dr2 sequences, and none of these mutants was generated by homologous recombination within the longer dr1 sequences. Thus, at least one of the wild-type copies of the dr1 element is preserved in each of these mutants. These results suggest that the RSV *td* mutants generated by homologous recombination within the dr1 sequences may be at a selective growth disadvantage compared with the wild-type virus. Alternatively, it is possible that additional compensatory mutations at sites in the RSV genome other than the dr regions must also occur in order for *td* mutants to replicate at wild-type levels. The reason for the inefficient replication of pSTD1 and pSTD2 is currently under investigation in our laboratory.

ACKNOWLEDGMENTS

We thank Mark Stinski and Stanley Perlman for critical reviews of the manuscript.

This research was supported by Public Health Service grant CA28051 from the National Cancer Institute.

REFERENCES

1. **Amendt, B. A., D. Hesslein, L.-J. Chang, and C. M. Stoltzfus.** 1994. Presence of negative and positive *cis*-acting RNA splicing elements within and flanking the first *tat* coding exon of human immunodeficiency virus type 1. Mol. Cell. Biol. **14:**3960–3970.
2. **Amendt, B. A., Z.-H. Si, and C. M. Stoltzfus.** 1995. Presence of exon splicing silencers within human immunodeficiency virus type 1 *tat* exon 2 and *tat-rev* exon 3: evidence for inhibition mediated by cellular factors. Mol. Cell. Biol. **15:**4606–4615.
3. **Amendt, B. A., S. B. Simpson, and C. M. Stoltzfus.** 1995. Inhibition of RNA splicing at the Rous sarcoma virus *src* 3′ splice site is mediated by an interaction between a negative *cis* element and a chicken embryo fibroblast nuclear factor. J. Virol. **69:**5068–5076.
4. **Arrigo, S., and K. Beemon.** 1988. Regulation of Rous sarcoma virus RNA splicing and stability. Mol. Cell. Biol. **8:**4858–4867.
5. **Berberich, S. L., and C. M. Stoltzfus.** 1991. Mutations in the regions of the Rous sarcoma virus 3′ splice sites: implications for regulation of alternative splicing. J. Virol. **65:**2640–2646.
6. **Bizub, D., R. A. Katz, and A. M. Skalka.** 1984. Nucleotide sequence of noncoding regions in Rous-associated virus-2: comparisons delineate conserved regions important in replication and oncogenesis. J. Virol. **49:**557–565.
7. **Coffin, J. M.** 1990. Retroviridae and their replication, p. 1437–1500. *In* B. N. Fields and D. M. Knipel (ed.), Virology. Raven Press, New York.
8. **Cullen, B. R.** 1991. Regulation of human immunodeficiency virus replication. Annu. Rev. Microbiol. **45:**219–250.

9. **Dirksen, W. P., R. K. Hampson, Q. Sun, and F. M. Rottman.** 1994. A purine-rich exon sequence enhances alternative splicing of bovine growth hormone pre-mRNA. J. Biol. Chem. **269:**6431–6436.
10. **Fu, X.-D., R. A. Katz, A. M. Skalka, and T. Maniatis.** 1991. The role of branchpoint and 3′-exon sequences in the control of balanced splicing of avian retrovirus RNA. Genes Dev. **5:**211–220.
11. **Gontarek, R. R., M. T. McNally, and K. Beemon.** 1993. Mutation of an RSV intronic element abolishes both U11/U12 snRNP binding and negative regulation of splicing. Genes Dev. **7:**1926–1936.
12. **Green, M. R.** 1991. Biochemical mechanisms of constitutive and regulated pre-mRNA splicing. Annu. Rev. Cell Biol. **7:**559–599.
13. **Katz, R. A., M. Kotler, and A. M. Skalka.** 1988. *cis*-acting intron mutations that affect the efficiency of avian retroviral RNA splicing: implication for mechanisms of control. J. Virol. **62:**2686–2695.
14. **Katz, R. A., and A. M. Skalka.** 1990. Control of retroviral RNA splicing through maintenance of suboptimal processing signals. Mol. Cell. Biol. **10:** 696–704.
15. **Linial, M., and D. Blair.** 1982. Genetics of retroviruses, p. 649–784. *In* R. Weiss, N. Teich, H. Varmus, and J. Coffin (ed.), RNA tumor viruses. Cold Spring Harbor Laboratory, Cold Spring Harbor, N.Y.
16. **Maniatis, T.** 1991. Mechanisms of alternative pre-mRNA splicing. Science **251:**33–34.
17. **McKeown, M.** 1992. Alternative mRNA splicing. Annu. Rev. Cell Biol. **8:**133–155.
18. **McNally, M. T., and K. Beemon.** 1992. Intronic sequences and 3′ splice sites control Rous sarcoma virus RNA splicing. J. Virol. **66:**6–11.
19. **McNally, M. T., R. R. Gontarek, and K. Beemon.** 1991. Characterization of Rous sarcoma virus intronic sequences that negatively regulate splicing. Virology **185:**99–108.
20. **Nelson, K. K., and M. R. Green.** 1989. Mammalian U2 snRNP has a sequence-specific RNA-binding activity. Genes Dev. **3:**1562–1571.
21. **Omer, C. A., K. Pogue-Geile, R. Guntaka, K. A. Staskus, and A. J. Faras.** 1983. Involvement of directly repeated sequences in the generation of deletions of the avian sarcoma virus *src* gene. J. Virol. **47:**380–382.
22. **Pathak, V. K., and H. M. Temin.** 1990. Broad spectrum of *in vivo* forward mutations, hypermutations, and mutational hotspots in a retroviral shuttle vector after a single replication cycle: deletions and deletions with insertions. Proc. Natl. Acad. Sci. USA **87:**6024–6028.
23. **Pulsinelli, G. A., and H. M. Temin.** 1991. Characterization of large deletions occurring during a single round of retrovirus vector replication: novel deletion mechanism involving errors in strand transfer. J. Virol. **65:**4786–4797.
24. **Reed, R.** 1989. The organization of 3′ splice site sequences in mammalian introns. Genes Dev. **3:**2113–2123.
25. **Rodcigno, R. F., M. Weiner, and M. A. Garcia-Blanco.** 1993. A mutational analysis of the polypyrimidine tracts of introns: effects of sequence differences in pyrimidine tracts on splicing. J. Biol. Chem. **268:**11222–11229.
26. **Sambrook, J., E. F. Fritsch, and T. Maniatis.** 1989. Molecular cloning: a laboratory manual, 2nd ed. Cold Spring Harbor Laboratory, Cold Spring Harbor, N.Y.
27. **Sanger, F., S. Niklen, and A. R. Coulson.** 1977. DNA sequencing with chain-terminating inhibitors. Proc. Natl. Acad. Sci. USA **74:**5463–5467.
28. **Smith, C. W. J., J. G. Patton, and B. Nadal-Ginard.** 1989. Alternative splicing in the control of gene expression. Annu. Rev. Genet. **23:**527–577.
29. **Sorge, J., W. Ricci, and S. H. Hughes.** 1983. *cis*-Acting RNA packaging locus in the 115-nucleotide direct repeat of Rous sarcoma virus. J. Virol. **48:**667–675.
30. **Staffa, A., and A. Cochrane.** 1994. The *tat*/*rev* intron of human immunodeficiency virus type 1 is inefficiently spliced because of suboptimal signals in the 3′ splice site. J. Virol. **68:**3071–3079.
31. **Stoltzfus, C. M.** 1988. Synthesis and processing of avian sarcoma retrovirus RNA. Adv. Virus Res. **35:**1–37.
32. **Stoltzfus, C. M., and S. J. Fogarty.** 1989. Multiple regions in the Rous sarcoma virus *src* gene intron act in *cis* to affect accumulation of unspliced RNA. J. Virol. **63:**1669–1676.
33. **Strohman, R., P. Moss, J. Micou-Eastwood, D. Spector, A. Przybyla, and B. Peterson.** 1977. Messenger RNA for myosin polypeptides: isolation from single myogenic cell cultures. Cell **10:**265–273.
34. **Tanaka, K., A. Watakabe, and Y. Shimura.** 1994. Polypurine sequences within a downstream exon function as a splicing enhancer. Mol. Cell. Biol. **14:**1347–1354.
35. **Temin, H. M.** 1993. Retrovirus variation and reverse transcription: abnormal strand transfers result in retrovirus genetic variation. Proc. Natl. Acad. Sci. USA **90:**6900–6903.
36. **Tsichlis, P. N., L. Donehower, G. Hager, N. Zeller, R. Malavarca, S. Astrin, and A. M. Skalka.** 1982. Sequence comparison in the crossover region of an oncogenic avian retrovirus recombinant and its nononcogenic parent: genetic regions that control growth rate and oncogenic potential. Mol. Cell. Biol. **2:**1331–1338.
37. **Voynow, S. L., and J. M. Coffin.** 1985. Evolutionary variants of Rous sarcoma virus: large deletion mutants do not result from homologous recombination. J. Virol. **55:**67–78.
38. **Wigler, M., A. Pellicer, S. Silverstein, and R. Axel.** 1978. Biochemical transfer of single-copy eukaryotic genes using total cellular DNA as donor. Cell **14:**725–734.
39. **Wu, J., and J. L. Manley.** 1989. Mammalian pre-mRNA branch site selection by U2 snRNP involves base pairing. Genes Dev. **3:**1553–1561.
40. **Xu, R., J. Teng, and T. A. Cooper.** 1993. The cardiac troponin T alternative exon contains a novel purine-rich positive splicing element. Mol. Cell. Biol. **13:**3660–3674.
41. **Yamamoto, T., J. S. Tyagi, J. B. Fagan, G. Jay, B. deCrombrugghe, and I. Pastan.** 1980. Molecular mechanism for the capture and excision of the transforming gene of avian sarcoma virus as suggested by analysis of recombinant clones. J. Virol. **35:**436–443.
42. **Yeakley, J. M., F. Hedjran, J.-P. Morfin, N. Merillat, M. G. Rosenfeld, and R. B. Emeson.** 1993. Control of calcitonin/calcitonin gene-related peptide pre-mRNA processing by constitutive intron and exon elements. Mol. Cell. Biol. **13:**5999–6011.
43. **Zamore, P. D., and M. R. Green.** 1992. Cloning and domain structure of the mammalian splicing factor U2AF. Nature (London) **355:**609–614.
44. **Zhang, L., and C. M. Stoltzfus.** 1995. A suboptimal *src* 3′ splice site in necessary for efficient replication of Rous sarcoma virus. Virology **206:**1099–1107.
45. **Zhuang, Y., A. M. Goldstein, and A. M. Weiner.** 1989. UACUAAC is the preferred branch site for mammalian mRNA splicing. Proc. Natl. Acad. Sci. USA **86:**2752–2756.